Numerical Study of a High-Pressure Turbine Stage with Inlet Distortions

Marco Bicchi[1, a)], Lorenzo Pinelli[1, b)], Michele Marconcini[1], Paolo Gaetani[2] and Giacomo Persico[2]

[1]*Department of Industrial Engineering, Università degli Studi di Firenze, Via di S. Marta 3, 50139 Firenze, Italy.*
[2]*Energy Department, Politecnico di Milano, Via Lambruschini 4, 20158 Milano, Italy.*

[a)] marco.bicchi@stud.unifi.it
[b)] lorenzo.pinelli@unifi.it

Abstract The study of inlet flow distortion (hot streaks and entropy waves) propagation through high-pressure turbine (HPT) stages is an open topic for aero-engine design, due to their multiple effects on aerodynamics, heat exchange and noise generation. The request to design compact and lightweight systems has recently led to a reduction of the combustor-turbine axial gap, making the interaction between the HPT and the combustor extremely critical. For this reason, the main aim of the present work is to numerically study how different clocking positions between temperature distortions and stator vanes can affect the evolution of hot streaks and entropy waves. In order to validate the numerical results, experimental data coming from an un-cooled high-pressure gas turbine stage tested at the *Laboratorio di Fluidodinamica delle Macchine* (LFM) of the *Politecnico di Milano* (Italy) has been used. The good agreement between numerical results and experimental data confirms the accuracy of the approach based on the CFD TRAF code and suggests recommendations for the design of the following rows.

INTRODUCTION

The interaction between combustor and turbine has been studied since the early 1980s [1] and nowadays it is still a very topical issue due to its effects on aerodynamics, heat exchange and turbomachinery noise production [2]. The development of high-performance low emission aero-engines represents an ongoing challenge. For this reason, the combustor-turbine axial gap has been reduced in order to create more compact and light systems. Due to this, the combustor-turbine interaction has become a critical problem, forcing researchers to investigate the evolution of hot streaks (HSs) and entropy waves (EWs), which turn out to be the main distortions coming from the combustor and entering the high-pressure turbine. The HSs are temperature spatial distortions produced by the presence of concentrated flames around the injection system, while the EWs are temperature space-time distortions caused by the combustion fluctuations. The HSs, due to the short length of the combustor and the flow structures, do not mix optimally, causing negative effects on the downstream turbine stages. In fact, the presence of HSs in an HPT can produce load and efficiency variations, forced vibrations, additional secondary flows and, finally, increased rotors heat exchange due to the cross-flow mechanism from the suction side to the pressure side, known as "positive jet" [3-9]. However, this last negative aspect can be reduced by appropriately selecting the number of stators and rotors [10]. On the other hand, the EWs have become very important with the introduction of low NO_x combustors suitable to match pollution requirements. Those burners use lean premixed flames which are particularly prone to instability and equivalence ratio fluctuations [11-16], leading to the generation of EWs which, in turn, produce additional indirect core noise.

Summarizing, the burner temperature distortions, together with the pressure and flow angle variations, act on the turbine blades as external forces. They produce local overheating, indirect core noise and aeromechanical and thermal fatigue failures. In this context, recent studies [17-19] have shown how the relative position between hot spots and first-stage stators can attenuate or enhance the interaction of distortions with subsequent rows. For this reason, in order

74th ATI National Congress
AIP Conf. Proc. 2191, 020020-1–020020-9; https://doi.org/10.1063/1.5138753
Published by AIP Publishing. 978-0-7354-1938-4/$30.00

to highlight the clocking effect between hot spots and stators, two different configurations are analysed with the URANS approach. In the first configuration HSs/EWs are injected directly on the stator leading edge (LE case), while in the second configuration they are injected at mid-pitch position between adjacent stators (MP case). Moreover, the clearance modelling effects are studied comparing resolved clearance simulations with modelled clearance analyses. An accurate resolution of the clearance flows is, in fact, necessary for predicting the correct evolution of HSs as widely described in the literature [20]. All the numerical simulations are validated against a dataset provided by the LFM of the *Politecnico di Milano*.

EXPERIMENTAL SETUP

The high-speed closed-loop test rig of the LFM is representative of an HPT first stage in subsonic conditions. Table 1 shows the main geometrical and operational parameters of the rig, while Figure 1 reports the meridian view of the rig (1a) and a picture of the stage (1b). The generator of HSs/EWs (EWG) was mounted two stator axial chords upstream of the stage at the 70% of the channel height. The EWG consists of 11 injectors producing temperature perturbations with an amplitude up to 20% of the mainstream temperature. The EWs are generated with a frequency of 30 Hz and the HSs are injected in mechanical equilibrium with the mainstream flow by imposing a suitable upstream pressure value. In this way the pressure disturbances caused by the injections are minimized. However, the size of the injector produces highly turbulent regions close to the jet which may promote the diffusion of HSs and EWs during their transport. Finally, to obtain experimental results consistent with a real stage behaviour proper sealings are employed to prevent any stator hub leakage and a rotor tip clearance of 1% of the blade height is present.

TABLE 1. Geometrical and operative stage parameters.

Parameters	Stator	Rotor
Reynolds number	0.87×10^6	0.50×10^6
Outlet Mach number	0.59	0.45
Solidity	1.20	1.25
Aspect Ratio	0.83	0.91
Blade number	22	25
Angular speed [rpm]	-	7000
Stage expansion ratio	1.4	
Inlet total temperature [K]	323	

(a) (b)

FIGURE 1. Meridional view of the test rig (a) and stage picture (b).

Figure 1a also shows the planes T_0, T_1 and T_2 where the experimental data were acquired. The T_0 plane was placed at one axial stator chord upstream of the stage, the T_1 plane at 32% of the axial stator chord downstream of the stators and T_2 at 32% of the axial rotor chord behind the stage. Detailed information concerning the test rig and the measurement techniques can be found in [21].

NUMERICAL SETUP

CFD simulations have been performed using the TRAF code [22], which is a three-dimensional viscous solver based on the finite volume method for the solution of Reynolds-Averaged Navier-Stokes equations on multi-block structured grids. A 2nd order Roe's upwind scheme TVD-MUSCL is adopted for the discretization of convective flows, while a central difference scheme for viscous flows. The turbulence closure is obtained by employing the Wilcox's k-

ω model in its high-Reynolds formulation [23]. A dual time-stepping multi-grid approach based on the 4-step Runge-Kutta scheme [24, 25] is used for time discretization (the highest blade passing frequency has been discretized with 25 physical time-steps) and a high level of code parallelization is achieved through a hybrid openMP/MPI architecture [26]. Moreover, the link between consecutive rows is handled with a sliding interface approach and a linear interpolation of the flow variables is employed.

The computational domain has been discretized using O-type grids for the stator and rotor blocks, while the remaining blocks have been obtained with H-type grids (Figure 2a). For the computations with resolved clearance, two additional O-type blocks were added in the clearance gap (Figure 2b), while a clearance model is used for the remaining simulation (modelled clearance). In such model, the flow variables are directly transferred from both sides of the blade surface in the clearance area, without resolving the leakage flow in the gap. An overall mesh of 11 million elements is generated for RANS simulations whereas for the full annulus URANS simulations the domain is extended to the whole wheel in order to avoid any blade count modification. In the full-annulus simulations the total number of elements is about 170 million.

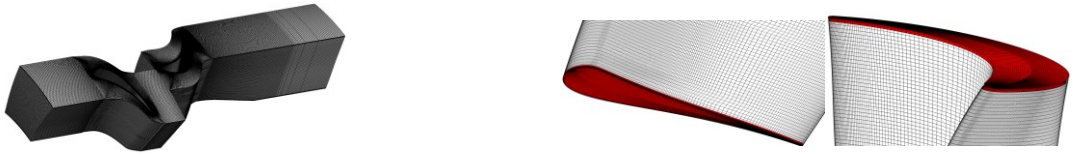

(a) (b)

FIGURE 2. A single sector of the multi-block spatial discretization (a) and highlighted blocks for clearance discretization (b).

RESULTS

In this section the main results obtained from numerical simulations and their comparison with measurements taken at *Politecnico di Milano* are reported. The results are shown in the following order: firstly, the simulations without any inlet disturbances are reported, then the computations with HSs and finally the analyses with EWs. Simulations with resolved clearance was not extended to URANS cases because of the lower robustness of this numerical setup.

No disturbance simulations

Stator exit – plane T_1

Figure 3 shows the comparison between the experimental contours of the total pressure loss coefficient (3a) and the numerical distributions (3b, 3c and 3d) from RANS e URANS analyses. Figure 3 highlights how the secondary loss cores are properly reproduced, and the wakes show a higher diffusion. This behaviour can be ascribed to the use of two equations turbulence models, but it can be also justified knowing that in the analysis of stator-rotor interaction the effects of interference between blades can increase the wake instability [21]. Different clearance models are also used at the stator hub to model a small leakage region present at the stator trailing edge. In the resolved clearance RANS case (3c), at 15% of the span, the loss core appears more pronounced than the solution with modelled clearance. This proves that a simplified clearance model is not able to completely reproduce the leakage flow effects of this small gap in the rear part of the stator at the hub.

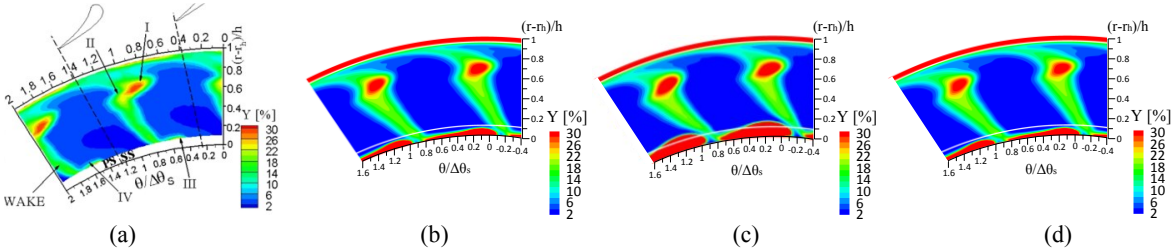

(a) (b) (c) (d)

FIGURE 3. Total pressure loss coefficient maps (plane T_1): (a) measured data, (b) RANS with modelled clearance, (c) RANS with resolved clearance and (d) URANS with modelled clearance.

Rotor exit – plane T_2

Figure 4 shows the total relative pressure coefficient maps. The figure contains the experimental data and the RANS and URANS simulation results with the two different clearance treatments. Comparing the distributions (4a) and (4d), it can be seen how the mean solution coming from the modelled clearance URANS simulation well reproduces the measurement of the relative total pressure loss. In addition, the loss core of the tip leakage vortex and its interaction with the tip passage vortex are accurately captured. On the contrary, considering the maps (4b) and (4c), the RANS simulations are not so accurate, especially at midspan where the wake is less diffused than the experimental case.

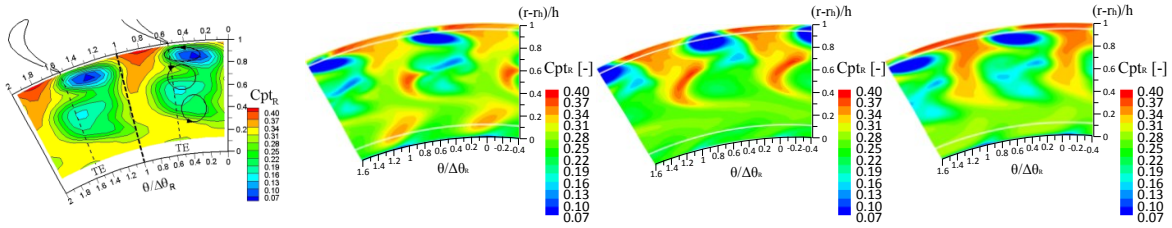

FIGURE 4. Relative total pressure coefficient Cpt_R maps (plane T_2): (a) measured data, (b) RANS with modelled clearance, (c) RANS with resolved clearance and (d) URANS with modelled clearance.

Hot streak simulations

For the HS simulations, non-uniform boundary conditions were imposed on the T_0 plane in accordance with the experimental data. The boundary conditions for the LE and MP cases included 2D maps of total temperature, total pressure, yaw and pitch angles, turbulent kinetic energy and turbulent length scale. A total temperature peak 1.2 times higher than the main flow, an 8% turbulence intensity (against 2.5% in the freestream) and a turbulent length scale equal to 0.18 of the channel height (against 0.01 of the freestream) were imposed at the spot center. Although these values are not representative of the first stage of an HPT in absolute terms, they are correct in relative terms. This simplification is due by the fact that it is difficult to reproduce the typical flow rates of the HPT first stage in a cold-flow test rig. Direct tests on real combustion chamber/turbine setup, on the contrary, suffer from too high temperature level for the instrumentation. The results for the LE and MP cases obtained with the RANS and URANS simulations are shown below.

Stator exit – plane T_1

Figures 5 and 6 show on the T_1 plane the experimental total temperature distribution for the leading edge and mid-pitch injection and the corresponding RANS numerical maps with modelled and resolved clearance. Generally, a good agreement between simulations and measurements is achieved, both in terms of HS positions and structures. In both cases, the total temperature peak attenuates to 105% of the mainstream temperature. However, in the LE modelled clearance simulation, the spot exhibits a more intense core and a lower diffusion in the spanwise direction with respect to the experimental one. Although the high temperature region is still too large, the resolved clearance case has a more similar spanwise diffusion. It is supposed that the interactions between wakes, secondary flows and HSs are not completely reproduced. A more detailed study of the leakage flow effects on HS propagation is thus necessary. Besides, the modelling of the injectors upstream of the stage (so far treated in terms of flow and turbulence non-uniform distributions) requires to be further investigated. Anyway, with reference to the mid-pitch case, the simulations correctly capture the HS migration towards the blade suction side in the upper part near the casing. This deviation is a result of the interaction between tip passage vortex and HSs [27].

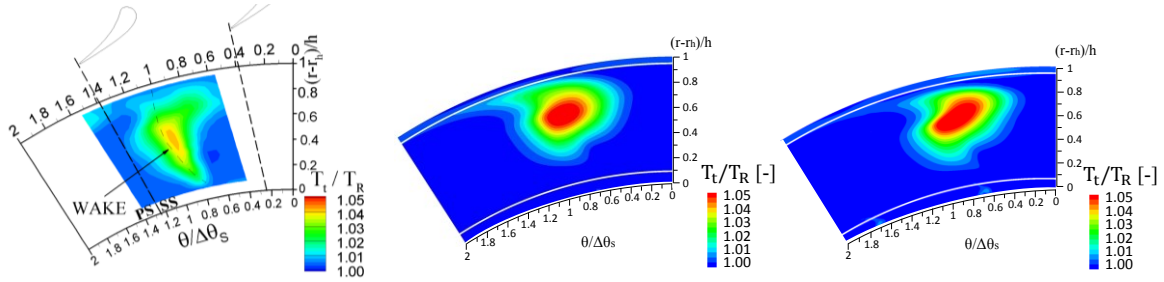

(a) (b) (c)

FIGURE 5. Total temperature maps on plane T_1 (LE case): (a) measured data, (b) RANS with modelled clearance and (c) RANS with resolved clearance.

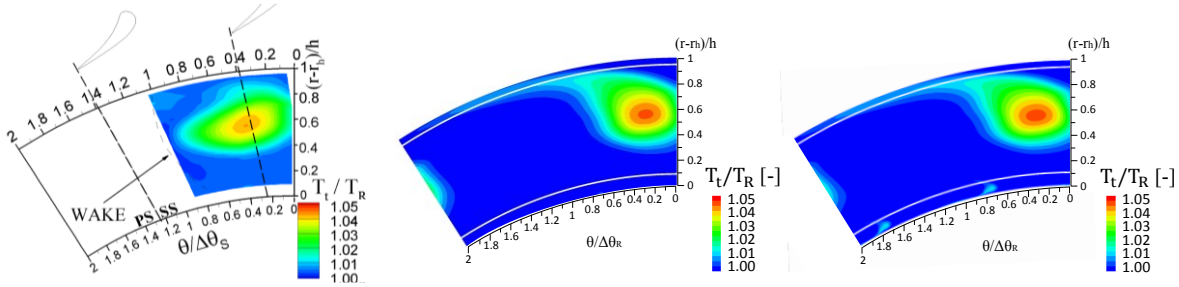

(a) (b) (c)

FIGURE 6. Total temperature maps on plane T_1 (MP case): (a) measured data, (b) RANS with modelled clearance and (c) RANS with resolved clearance.

Figure 7 shows the total pressure loss coefficient contours on the T_1 plane. In both cases (LE and MP) a modulation and redistribution of secondary losses is observed compared to the undisturbed case. The modulation is accentuated in the MP case because the turbulent HS spots inhibit the cross-flow mechanism that improves the secondary flows. On the contrary, in the LE case the interaction between turbulent spots and cross-flows is negligible, so that no significant attenuation is noticed [21]. The above statements are confirmed by looking at the turbulent kinetic energy (TKE) contours on the blade-to-blade plane at 70% of the span (Figure 7).

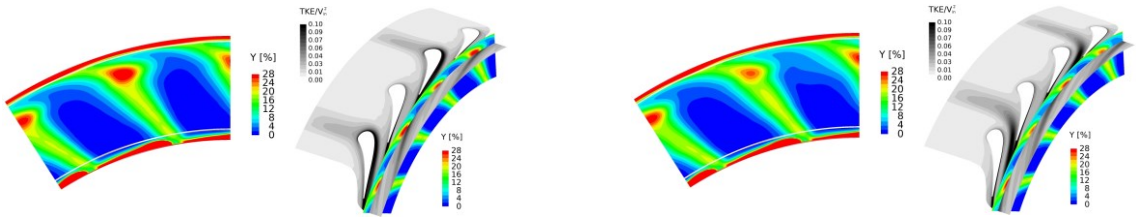

(a) (b)

FIGURE 7. Total pressure loss coefficient and turbulent kinetic energy maps (plane T_1): (a) LE and (b) MP cases.

Rotor exit – plane T_2

Figure 8 shows, for the LE case, both the experimental contours of total temperature averaged over time (8a) and the same quantity coming from the URANS simulation with modelled clearance (8b). The two maps (obtained in the fixed reference system) exhibit a good agreement between experimental and numerical values. A total temperature spanwise stratification caused by the dislocation of the underturning and overturning regions, connected to different work extraction, is observed. On the contrary, in pitchwise direction the distribution appears more uniform notwithstanding the presence of the stator wake/HS avenue phenomenon. The temperature of the HSs attenuates to 94% of the mainstream temperature. Looking at the instantaneous fields downstream of the stage (not reported for brevity) a 120° pseudo-periodicity emerges caused by the interaction between the stator/rotor rows and related to the

blade count. Finally, Figure 8c shows the total temperature pattern repeated 11 times (such as the number of injectors) at the rotor exit. This spatial distribution can be extremely useful to define the best circumferential positioning of the second-stage stators. In fact, exposing the blades to a lower time-average temperature spot can improve their life [1].

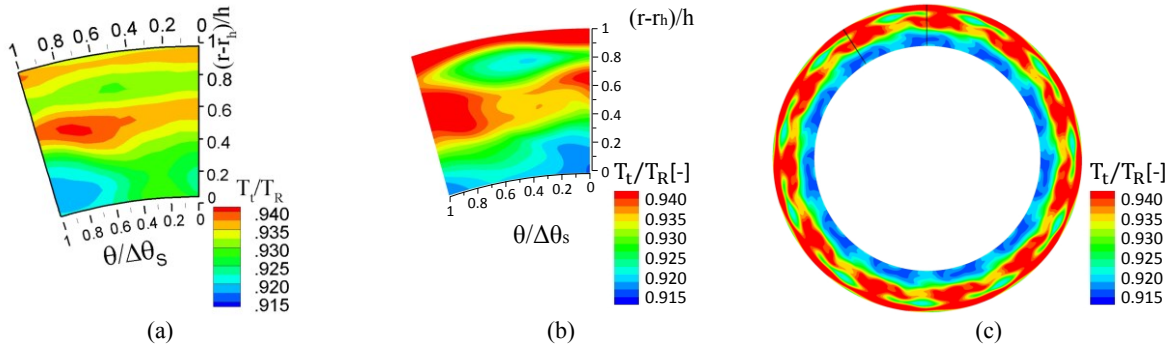

FIGURE 8. Total temperature maps on plane T_2 (LE case): (a) measured data, (b) single pattern and (c) full-annulus obtained from URANS simulation with modelled clearance.

Entropy wave simulations

The EWs can be described as time-varying HSs that pulsate periodically [28] and thus boundary conditions similar to the HS simulations were imposed on the T_0 plane over time. In particular, the inlet values oscillated with the injector frequency to replicate the EW spots. In the following paragraphs the instantaneous results provided by the URANS simulations with modelled clearance are reported.

Stator exit – plane T_1

Figures 9 and 10 show the instantaneous temperature contours on the T_1 plane for the MP case (the LE case is not reported for the sake of brevity) at 8 equally-spaced instant of a single EW fluctuation: it can be observed how the sinusoidal trend of the EWs imposed at the inlet is still present downstream of the stator row. In fact, from the 1st to the 5th frame the spots increase their intensity, while from the 5th to the 8th frame the core temperature of the spots decreases. In both cases (LE and MP) the total temperature peak is about 12 K lower than the one with HSs. This implies lower thermal loads on the following row. In particular, the greatest reduction is evident in the MP case, but detailed investigations are still ongoing. Besides, more in-depth studies are still necessary to evaluate the thermal load fluctuation on the blades as heat transfer is not considered in all the simulations (adiabatic blade surfaces).

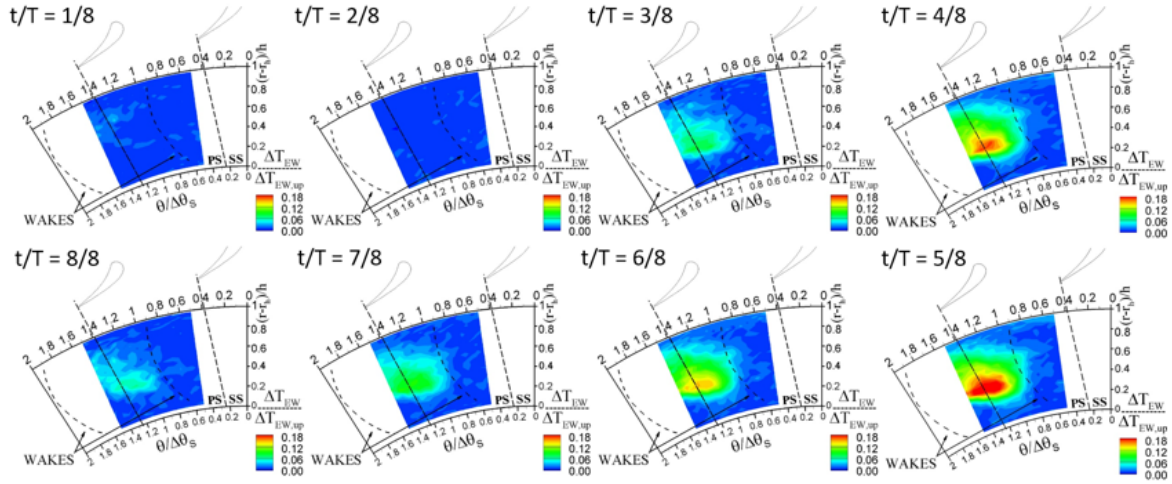

FIGURE 9. Instantaneous experimental maps of total temperature on plane T_1 (MP case).

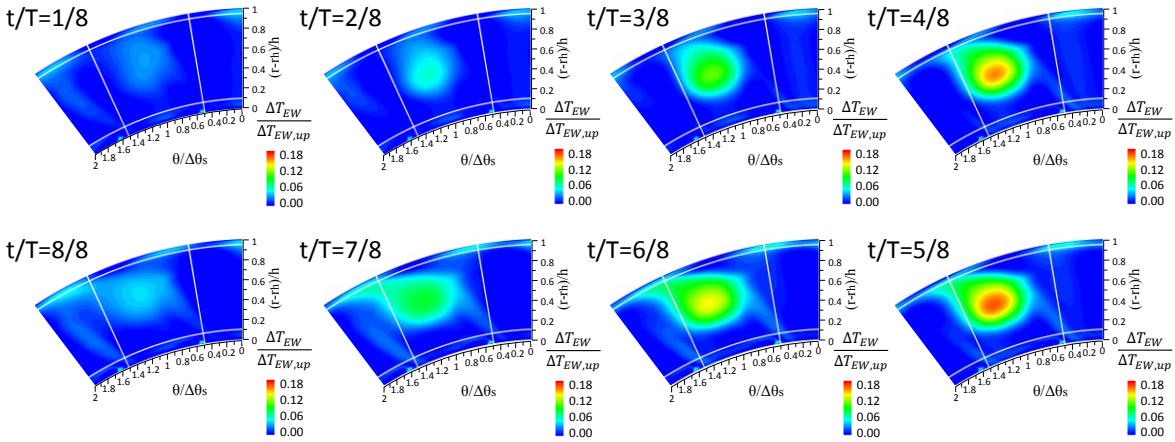

FIGURE 10. Instantaneous numerical maps of total temperature on plane T_1 (MP case).

Comparing the experimental maps with the numerical ones (Figures 9 and 10) a good agreement is observed both in terms of shape and intensity of the spots. This confirms the robustness of the implemented numerical setup and shows once again the importance of combining experimental measurements with numerical simulations to better understand the EW evolution thought an HPT stage.

Rotor exit – plane T_2

Figure 11 shows the instantaneous numerical map of the total temperature in the fixed reference system downstream of the rotor row (only the MP case is reported for coherence with the results shown above): it must be remarked that the temperature field is determined by the work extraction and by the EW evolution. Passing through the stage, for both cases (LE and MP) the total temperature fluctuation attenuates to 96% of the mainstream temperature. The 25 traces of the rotor blades are clearly present at the different instants and interact with the EW spots. These tracks are characterized by a high temperature region (from 75% to 100% of the span) and a low temperature region (from 30% to 70%): the periodic modulation among the different channel and time frames of such temperature field is due to the interaction with the pulsating EW. Although the field downstream of the stage is more uniform than at the stator exit, the presence of such structures can cause periodic changes in blade load and heat exchange on the following stators. These fluctuations can thus affect the blade aerodynamic performance and the cooling system behaviour. Again, as in the HS cases, a 120° pseudo-periodicity is observed due to the stage stator/rotor interaction.

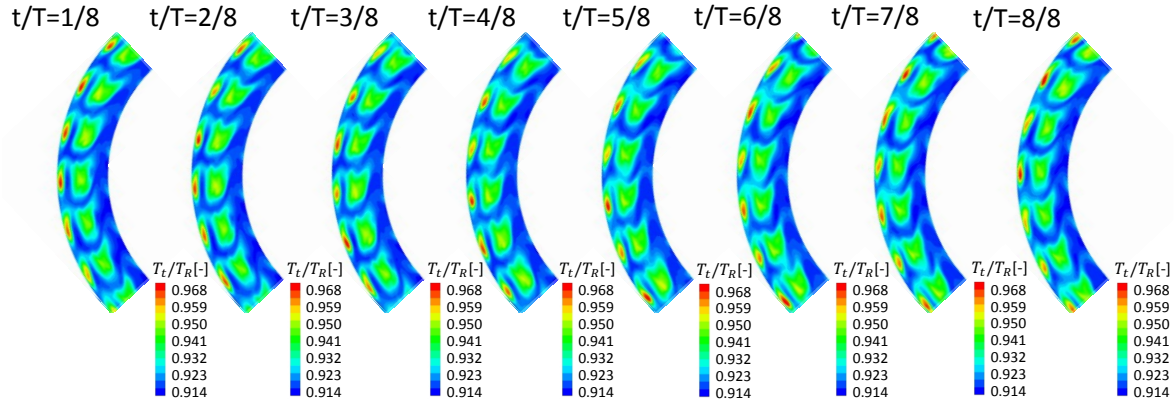

FIGURE 11. Instantaneous total temperature maps on plane T_2 (MP case).

CONCLUSIONS

The combustor-turbine interaction is a current topic and thus many numerical and experimental applications are devoted to investigating this phenomenon. In this context, the partnership with the *Politecnico di Milano* led to the development of a numerical setup able to accurately predict the HS and EW evolution through an HPT stage.

Initially, undisturbed RANS analyses have been carried out with the purpose of studying the stage aerodynamics. Two spatial discretizations have been used, the first one with a model to predict clearance flows and the other one with treatment complete discretization of the clearance gap with dedicated mesh blocks. The simplified clearance model reduces the number of elements and provides a more robust setup. Nonetheless, the resolved clearance approach better reproduces the interaction between the leakage and main flow. As a result, the main differences have been pinpointed close to the clearance zones. Moreover, a no disturbance URANS analysis with modelled clearance has been performed as well. Comparing the unsteady average results with the previous ones, no glaring discrepancies have been observed downstream the stators. Conversely, some differences have been noted behind the rotor row, where the time-average URANS solution shows a better agreement.

Subsequently, the study of HS evolution has been started with RANS techniques. The effects of the clocking position between injectors and stators have been evaluated for both LE and MP cases. Then, two further URANS analyses have been performed to increase the prediction accuracy. It has been noticed how behind the stator row the HS injection induced an altered temperature field compared to the undisturbed case. Moreover, besides it has been observed a pronounced attenuation of the HSs downstream of the stator, the HSs can anyhow affect the rotor durability and the cooling system efficiency. Different HS spot shapes have been observed depending on the injection position. Comparing the numerical results, the highest effect has been recorded for the LE case. Nevertheless, in the MP configuration the secondary losses exhibit a greater variation compared to the undisturbed case. Likely the latter effect has been induced by the turbulent flow migration close to the endwalls, which affects the secondary flow generation. Concerning the heat exchange, the LE case results the most critical position, while the pressure losses are similar between the two cases (an average value of 7.8% with a maximum deviation of ± 0.017%). Despite the presence of complex flow structures, the simulations provide results consistent with the experimental data, capturing the main differences between the configuration with and without inlet distortions. The influence of the injection position to the temperature maps at the stage exhaust (Figure 8c) is extremely attractive. Ideally, a systematic optimization of the injector position will be possible in the future, keeping the thermal load on the 2nd stage stators to a minimum and thus increasing the blade durability.

Finally, two last URANS simulations (LE and MP cases) with EWs have been carried out for a faithful representation of the combustor-turbine interaction in a modern aero-engine. These analyses have shown how, downstream of the stator row, the temperature fluctuations basically preserve the inlet trend. Moreover, the MP case produces a lower thermal load on the stator row than the HS case, in accordance with the HS simulation results. Nevertheless, the total temperature maps behind at the stage exhaust are similar in both cases, with well-defined but not very intense regions of high temperature.

In conclusion, the combination of experimental measurements and numerical simulations turns out to be a fundamental procedure to obtain useful suggestions for the design of the first stage of an HPT. However, more insight on clearance flows and on different injection configurations deserve to be studied in the future works.

REFERENCES

1. D. J. Dorney et al., “A Survey of Hot Streak Experiments and Simulations,” in *International Journal of Turbo and Jet Engines*, Vol. 16 (1), pp. 1–16, (De Gruyter, 1999).
2. L. Pinelli et al., “On the Numerical Evaluation of Tone Noise Emissions Generated by a Turbine Stage: An In-depth Comparison Among Different Computational Methods”, in *ASME Turbo Expo: Power for Land, Sea, and Air*, Vol. 2B: Turbomachinery, pp. V02BT41A002, doi:10.1115/GT2015-42376 (ASME, 2015).
3. L. He et al. “Effect of Hot-Streak Counts on Turbine Blade Heat Load and Forcing,” in *Journal of Propulsion and Power*, Vol. 23 (6), pp. 1235–1241, (AIAA, 2007).
4. W. R. Hawthorne, “Rotational Flow through Cascades Part I: The Components of Vorticity,” in *The Quarterly Journal of Mechanics and Applied Mathematics*, Vol. 8 (3), pp. 266–279, (Oxford University Press, 1955).
5. B. Lakshminarayana and J. H. Horlock, “Generalized Expressions for Secondary Vorticity Using Intrinsic Co-ordinates,” in *Journal of Fluid Mechanics*, Vol. 59 (1), pp. 97–115, (Cambridge University Press, 1973).

6. T. L. Butler, O. P. Sharma, H. D. Joslyn and R. P. Dring, "Redistribution of an Inlet Temperature Distortion in an Axial Flow Turbine Stage," in *Journal of Propulsion and Power*, Vol. 5 (1), pp. 64–71, (AIAA, 1989).
7. D. J. Dorney et al., "Unsteady Analysis of Hot Streak Migration in a Turbine Stage," in *Journal of Propulsion and Power*, Vol. 8 (2), pp. 520–529, (AIAA, 1992).
8. B. Krouthen and M. B. Giles, "Numerical Investigation of Hot Streaks in Turbines," in *Journal of Propulsion and Power*, Vol. 6 (6), pp. 769–776, (AIAA, 1990).
9. K. Zhou and C. Zhou, "Transport Mechanism of Hot Streaks and Wakes in a Turbine Cascade," in *Journal of Propulsion and Power*, Vol. 32 (5), pp. 1045–1054, (AIAA, 2016).
10. T. Shang and A. H. Epstein, "Analysis of Hot Streak Effects on Turbine Rotor Heat Load," in *Journal of Turbomachinery*, Vol. 119 (3), pp. 544–553, (ASME, 1997).
11. T. Lieuwen and B. T. Zinn, "The Role of Equivalence Ratio Oscillations in Driving Combustion Instabilities in Low NOx Gas Turbines," in *Symposium on combustion*, Vol. 27 (2), pp. 1809–1816, (Elsevier, 1998).
12. W. Polifke et al., "Constructive and Destructive Interference of Acoustic and Entropy Waves in a Premixed Combustor with a Choked Exit," in *Int. Journal of Acoustics and Vibration*, Vol. 6 (3), pp. 135–146, (2001).
13. J. G. Lee et al., "Measurement of Equivalence Ratio Fluctuation and Its Effect on Heat Release During Unstable Combustion," in *Proceedings of the Combustion Institute*, Vol. 28 (1), pp. 415–421, (Elsevier, 2000).
14. A. S. Morgans and I. Duran, "Entropy Noise: A Review of Theory, Progress and Challenges," in *International Journal of Spray and Combustion Dynamics*, Vol. 8 (4), pp. 285–298, (SAGE, 2016).
15. T. C. Lieuwen and V. Yang, "Combustion Instabilities in Gas Turbine Engines", (AIAA, 2005).
16. H. J. Lee, "Combustion Instability Mechanisms in a Lean Premixed Gas Turbine Combustor", Phd. thesis, 2009.
17. L. He et al., "Influence of Hot Streak Circumferential Length-Scale in Transonic Turbine Stage," in *ASME Turbo Expo 2004: Power for Land, Sea and Air*, pp. 1117–1126 (ASME, 2004).
18. D. J. Dorney and K. Gundy-Burlet, "Hot Streak Clocking Effects in a 1-1/2 Stage Turbine," in *ASME 1995 International Gas Turbine and Aeroengine Congress and Exposition*, pp. V001T01A059, (ASME, 1995).
19. S. Murari, et al. "CFD Analyses of a Single Stage Turbine With Inlet Hot-Streak at Different Circumferential Locations," in *ASME Turbo Expo 2013: Turbine Technical Conference and Exposition*, (ASME, 2013).
20. D. J. Dorney and D. L. Sondak, "Effects of Tip Clearance on Hot Streak Migration in a High-Subsonic Single-Stage Turbine," in *Journal of Turbomachinery*, Vol. 122 (4), pp. 613–620, (ASME, 2000).
21. P. Gaetani et al., "Computational and Experimental Study of Hot Streak Transport Within the First Stage of a Gas Turbine," *ASME paper* GT2019-91276.
22. A. Arnone, "Viscous Analysis of Three–Dimensional Rotor Flow Using a Multigrid Method," in *ASME Journal of Turbomachinery*, Vol. 116 (3), pp. 435–445, (ASME, 1994).
23. D. C. Wilcox, "Turbulence Modeling for CFD," 2nd ed. DCW Ind. La Canada, CA, 1998.
24. A. Arnone et al., "Integration of Navier–Stokes Equations Using Dual Time Stepping and a Multigrid Method," in *AIAA Journal*, Vol. 33 (6), pp. 985–990, (AIAA, 1995).
25. A. Jameson, "Time Dependent Calculations Using Multigrid With Applications to Unsteady Flows Past Airfoils and Wings," in *10th Computational Fluid Dynamics Conference*, (AIAA, 1991).
26. M. Giovannini et al., "A Hybrid Parallelization Strategy of a CFD Code for Turbomachinery Applications," in *11th European Conference on Turbomachinery Fluid Dynamics and Thermodynamics*, Madrid 2015.
27. P. Gaetani and G. Persico, "Hot Streak Evolution in an Axial High Pressure Turbine Stage," in *International Journal of Turbomachinery, Propulsion and Power*, Vol. 2 (2), (Multidisciplinary Digital Publishing Institute, 2017).
28. P. Gaetani and G. Persico, "Transport of Entropy Waves Within a High Pressure Turbine Stage," in *ASME Journal of Turbomachinery*, Vol. 141 (3), pp. 031006-031006-9, doi:10.1115/1.4042165 (ASME, 2019).